HNPS Advances in Nuclear Physics

33rd Symposium of the Hellenic Nuclear Physics Society

Hellenic Nuclear Physics Society

HNPS Advances in Nuclear Physics

Editors:

T.J. Mertzimekis
P. Koseoglou

Proceedings of the 33rd Hellenic Symposium on Nuclear Physics and Applications

HNPS2025

National and Kapodistrian University of Athens

5 & 6 June 2025

A hybrid nuclear model approach for neutral-current inelastic neutrino-nucleus scattering

Dimitrios K. Papoulias, Matti Hellgren, Jouni Suhonen

Hellenic Nuclear Physics Society
Advances in Nuclear Physics
since 1990

ARTICLE

A hybrid nuclear model approach for neutral-current inelastic neutrino-nucleus scattering

D. K. Papoulias,[*,1] Matti Hellgren,[2,3] and Jouni Suhonen[2]

[1]Instituto de Física Corpuscular (IFIC), CSIC-Universitat de Valéncia, E-46980 Valencia, Spain
[2]University of Jyväskylä, Department of Physics, P.O. Box 35, FI-40014, Finland
[3]Current address: CEA, DES, IRESNE, DER, SPRC, F-13108 Saint Paul Lez Durance, France

[*]Corresponding author: dipapou@ific.uv.es

Abstract

We present nuclear structure calculations for neutral-current inelastic neutrino-nucleus scattering off the stable $^{203/205}$Tl isotopes using a novel hybrid approach combining the nuclear shell-model (NSM) and the microscopic quasiparticle-phonon model (MQPM). The hybrid model leverages the accuracy of NSM for low-lying states and the computational efficiency of MQPM for higher-energy excitations. We compute scattering cross sections as functions of incoming neutrino energy and nuclear recoil energy, and present event rates for various neutrino sources, including solar neutrinos, stopped-pion neutrinos, and diffuse supernova neutrino background. The results demonstrate the importance of inelastic channels, particularly at higher neutrino energies where they become competitive with coherent elastic neutrino-nucleus scattering.

Keywords: Neutrino-nucleus scattering; Hybrid model; Nuclear structure; Thallium isotopes; Inelastic scattering

1. Introduction

Neutrino-nucleus scattering is a key process for probing both fundamental neutrino properties and the nuclear structure. Recent experimental achievements, including the first observations of coherent elastic neutrino-nucleus scattering (CEνNS) exploiting neutrinos from stopped-pion-decay-at-rest (π-DAR) by the COHERENT Collaboration [1, 2], reactor anti-neutrinos by Dresden-II [3] and CONUS [4] Collaborations as well as solar neutrinos by PandaX-4T [5] and XENONnT [6] dark matter direct detection experiments, have stimulated interest in precise theoretical predictions of neutrino-nucleus interactions. While CEνNS dominates by several orders of magnitude at low momentum transfers, inelastic channels become increasingly important at higher energies. Thallium isotopes ($^{203/205}$Tl) are particularly relevant as they serve as dopant materials in several dark matter and neutrino detectors including COSINE-100 [7], DAMA/LIBRA [8], and others.

The theoretical description of inelastic scattering requires accurate nuclear structure calculations

across a wide energy range. Traditional approaches like the nuclear shell-model (NSM) excel at low energies but become computationally prohibitive for higher excitations. Conversely, quasiparticle-based models like the microscopic quasiparticle phonon model (MQPM) efficiently describe higher-energy states but lack precision for low-lying levels. In these proceedings, we present results from a novel hybrid (NSM+MQPM) nuclear model approach, first presented in [9], applied to inelastic neutrino scattering off thallium isotopes, extending previous shell-model only calculations performed in Ref. [10]. Moreover the results are presented in terms of a new formalism based on the nuclear recoil energy which constitutes the observable in CEνNS and dark matter direct detection searches.

2. Theoretical Framework

2.1 Hybrid Nuclear Model

The hybrid approach combines the NSM and MQPM to leverage their respective strengths. The former provides high accuracy for low-lying states. However, it is computationally expensive as a large-scale diagonalization is required. The present calculations are performed in the framework of jj56pn model space by adopting the *khhe* interaction. On the other hand, the MQPM provides a realistic description of the excitation spectrum up to energies that are entirely out of reach for the NSM, although the agreement with experiment for individual states is often only moderate. This limitation is especially critical in the case of low-energy neutrinos, where reliable predictions require both an accurate modeling of the strongly contributing low-lying excitations and a realistic description of the forbidden multipole transitions. As will become evident in the solar-neutrino results presented below, addressing both aspects simultaneously is essential.

To exploit the predictive power of both nuclear models, Ref. [9] introduced a hybrid nuclear model, combining NSM states below 3 MeV with MQPM states above this energy, in an effort to compute neutral-current (NC) transition densities as accurately as possible. Figure 1 illustrates a comparison of low-lying spectra of $^{203/205}$Tl obtained with NSM (top panel) and MQPM (bottom panel) compared to experimental data. As can be seen, although the MQPM reproduces the correct spin-parities for ground states and low-lying excitations, the energy levels show some discrepancies compared to experimental values. On the other hand the NSM is characterized by an enhanced predictive power, which however, is constrained to the lowest-lying states only. These two results highlight the need for the hybrid approach presented for the first time in [10] and summarized in these proceedings.

2.2 Formalism in terms of nuclear recoil energy

As is well known, any semi-leptonic nuclear process can be described within the framework of the Donnelly-Walecka formalism, where the effective Hamiltonian of the scattering process can be described in the lowest order as a current-current interaction

$$\hat{H}_{\text{eff}} = \frac{G_F}{\sqrt{2}} \int d^3\mathbf{x} \, j_\mu(\mathbf{x}) \mathcal{J}^\mu(\mathbf{x}), \tag{1}$$

where G_F is the Fermi constant while j_μ ($\mathcal{J}_\mu$) represents the leptonic (hadronic) current. In the case of NC inelastic neutrino-nucleus scattering we are interested in this work, the double-differential cross section for a transition from initial state $|i\rangle$ to final state $|f\rangle$, with excitation energy $\omega = E_\nu - E_{\nu'}$ with E_ν ($E_{\nu'}$) being the initial (final) neutrino energy, can be shown to be [11–13]

$$\frac{d^2\sigma_{i \to f}}{d\Omega d\omega} = \frac{G^2 |\mathbf{k}'| E_{\nu'}}{\pi(2J_i + 1)} \left(\sum_{J \geq 0} \sigma_{\text{CL}}^J + \sum_{J \geq 1} \sigma_{\text{T}}^J \right), \tag{2}$$

where $\mathbf{k}'$ denotes the 3-momentum of the outgoing neutrino while σ_{CL}^J (σ_{T}^J) represents the Coulomb-longitudinal (transverse) contribution. The latter are written in terms of the Coulomb ($\hat{\mathcal{M}}$), longi-
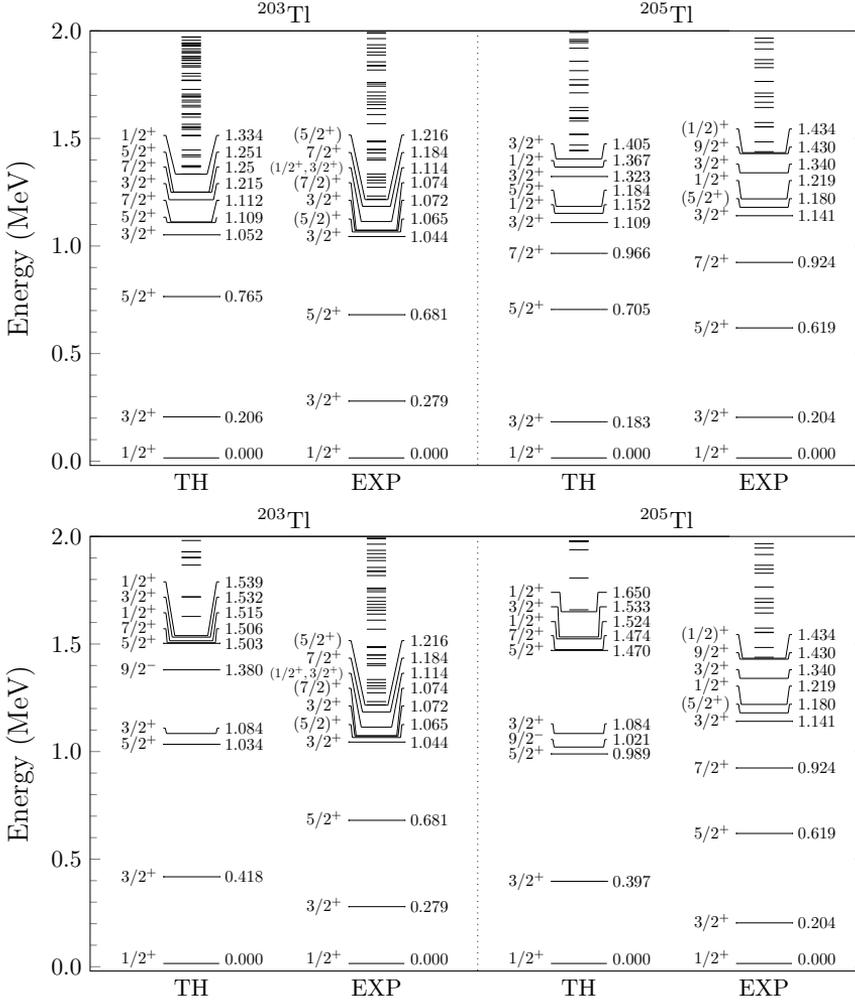
Figure 1. Low-lying spectra of $^{203/205}$Tl calculated with NSM [10] (top) and MQPM [9] (bottom). A comparison with experimental data is also given.

tudinal ($\hat{\mathcal{L}}$), transverse electric ($\hat{\mathcal{T}}^{\text{el}}$) and transverse magnetic ($\hat{\mathcal{T}}^{\text{mag}}$) nuclear operators [12], as

$$
\sigma_{\text{CL}}^J = (1 + \cos\theta)|(J_f||\hat{\mathcal{M}}_J(q)||J_i)|^2 + \left(1 + \cos\theta - 2\frac{E_\nu E_{\nu'}}{q^2}\sin^2\theta\right)|(J_f||\hat{\mathcal{L}}_J(q)||J_i)|^2
$$
$$
+ \frac{E_\nu - E_{\nu'}}{q}(1 + \cos\theta)2\text{Re}\left[(J_f||\hat{\mathcal{L}}_J(q)||J_i)(J_f||\hat{\mathcal{M}}_J(q)||J_i)^*\right]
\tag{3}
$$

$$
\sigma_{\text{T}}^J = \left(1 - \cos\theta + \frac{E_\nu E_{\nu'}}{q^2}\sin^2\theta\right)\left[|(J_f||\hat{\mathcal{T}}_J^{\text{el}}(q)||J_i)|^2 + |(J_f||\hat{\mathcal{T}}_J^{\text{mag}}(q)||J_i)|^2\right]
$$
$$
- \frac{(E_\nu - E_{\nu'})}{q}(1 - \cos\theta)2\text{Re}\left[(J_f||\hat{\mathcal{T}}_J^{\text{mag}}(q)||J_i)(J_f||\hat{\mathcal{T}}_J^{\text{el}}(q)||J_i)^*\right].
\tag{4}
$$

To achieve a direct comparison with experimentally measurable quantities, in Ref. [10] the cross

section has been expressed, for the first time, in terms of nuclear recoil energy T, as

$$\frac{\mathrm{d}\sigma}{\mathrm{d}T} = \frac{\mathrm{d}\sigma}{\mathrm{d}\cos\theta} \frac{M}{E_\nu(E_\nu - \omega)}, \tag{5}$$

with M being the nuclear mass while the recoil energy is approximately given by

$$T \approx \frac{E_\nu(E_\nu - \omega)(1 - \cos\theta) + \omega^2/2}{M}, \tag{6}$$

under the approximations of $T \ll E_\nu$ and $T \ll M$. It is worth noticing that the above expressions in the limit $\omega \to 0$ are reduced to those obtained in Ref. [14] for the case of CEνNS. Analytical expressions for the relevant kinematic terms appearing in Eq. (2) can be derived, and read [10]

$$\sum_{\text{spins}} l_0 l_0^* = \frac{4E_\nu^2 - 4E_\nu(T + \omega) - 2MT + \omega(2T + \omega)}{2E_\nu(E_\nu - \omega)}, \tag{7}$$

$$\sum_{\text{spins}} l_3 l_0^* = \frac{(T + \omega)\left(4E_\nu^2 - 2MT - 4E_\nu(T + \omega) + \omega(2T + \omega)\right)}{2\sqrt{2}E_\nu(E_\nu - \omega)\sqrt{MT}}, \tag{8}$$

$$\sum_{\text{spins}} l_3 l_3^* = \frac{(T + \omega)^2\left(4E_\nu^2 - 2MT - 4E_\nu(T + \omega) + \omega(2T + \omega)\right)}{4E_\nu MT(E_\nu - \omega)}, \tag{9}$$

$$\sum_{\text{spins}} \frac{1}{2}(\mathbf{l} \cdot \mathbf{l}^* - l_3 l_3^*) = \frac{(2MT - \omega(2T + \omega))\left(4E_\nu^2 + 2MT - 4E_\nu(T + \omega) + \omega(2T + \omega)\right)}{8E_\nu MT(E_\nu - \omega)}, \tag{10}$$

$$\sum_{\text{spins}} \frac{-i}{2}(\mathbf{l} \times \mathbf{l}^*)_3 = \frac{(2E_\nu - \omega)(2MT - \omega(2T + \omega))}{2\sqrt{2}E_\nu(E_\nu - \omega)\sqrt{MT}}, \tag{11}$$

by noting that the positive sign appearing in the leading term of $l_3 l_0^*$ given in Ref. [14] should be corrected by a minus sign as shown here. Moreover, the following interesting relations between the lepton traces can be obtained

$$\begin{aligned}
l_3 l_0^* &= \frac{T + \omega}{\sqrt{2MT}} l_0 l_0^* \approx \left(\frac{T + \omega}{q}\right) l_0 l_0^*, \\
l_3 l_3^* &= \frac{(T + \omega)^2}{2MT} l_0 l_0^* \approx \left(\frac{T + \omega}{q}\right)^2 l_0 l_0^*,
\end{aligned} \tag{12}$$

offering better insight into their relative contributions to the cross section. It becomes evident that the $l_3 l_0^*$ ($l_3 l_3^*$) term is suppressed (doubly suppressed) compared to $l_0 l_0^*$ since for low-energy neutrino-nucleus scattering one has $T \ll \omega$ and $\omega/q \approx 10\%$ or less. To be concrete, q is in the range 10–40 MeV, ω varies within 1.1–11.8 MeV for ^{205}Tl (1.3–19.2 MeV for ^{203}Tl), while T is of the order of a few keV. Therefore, in Eq. (2) one expects the terms proportional to $l_3 l_0^*$ and $l_3 l_3^*$ to contribute minimally. For completeness, let us also note that for very tiny recoil energies, i.e., $T \to T_{\min}$, it holds that $\omega \approx q$, implying that $l_3 l_0^* \approx l_3 l_3^* \approx l_0 l_0^*$. However, the latter case is practically irrelevant in neutrino-scattering and dark matter direct detection experiments. On the other hand, the leptonic trace $(\mathbf{l} \cdot \mathbf{l}^* - l_3 l_3^*)$ can be expressed in terms of $l_0 l_0^*$ as follows

$$(\mathbf{l} \cdot \mathbf{l}^* - l_3 l_3^*) = \left(1 - \frac{\omega(2T + \omega)}{2MT}\right)\left(l_0 l_0^* + \frac{2MT}{E_\nu(E_\nu - \omega)}\right), \tag{13}$$

simplifying further to

$$(\mathbf{l} \cdot \mathbf{l}^* - l_3 l_3^*) \approx \left(1 - \frac{\omega^2}{q^2}\right)\left(l_0 l_0^* + \frac{q^2}{E_\nu \left(E_\nu - \omega\right)}\right). \tag{14}$$

Finally, for the typical keV-order recoil energies, detectable in rare event experiments, it holds that $1 - (\omega/q)^2 \approx 1$, and hence $(\mathbf{l} \cdot \mathbf{l}^* - l_3 l_3^*) \approx l_0 l_0^* + \frac{q^2}{E_\nu(E_\nu - \omega)}$, i.e., it is always larger than $l_0 l_0^*$, with the only exception being the case of extremely tiny recoil energies for which one has $(\mathbf{l} \cdot \mathbf{l}^* - l_3 l_3^*) \ll l_0 l_0^*$.

3. Results and Discussion

In this section we proceed by presenting the main outcomes of this work. We begin by showing in Fig. 2 the relative strength of the Coulomb-longitudinal and transverse operators to the total inelastic neutrino-$^{203/205}$Tl cross section as a function of the incoming neutrino energy. In both cases we find that the transverse terms dominate across all neutrino energies.
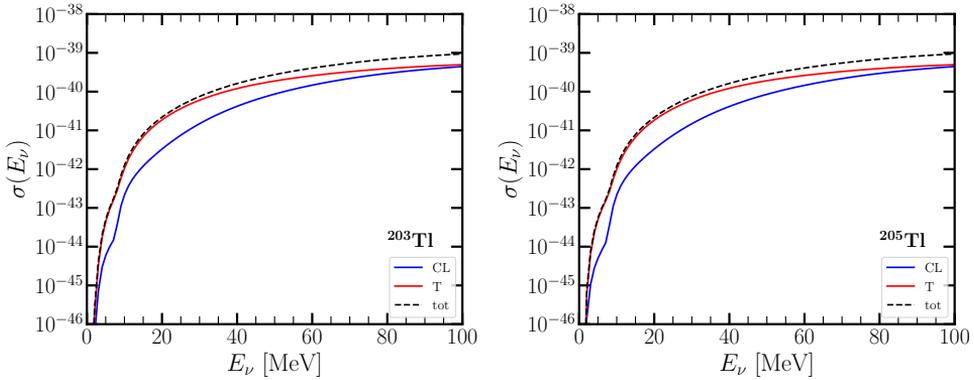

Figure 2. Contribution of Coulomb-longitudinal and transverse terms to the inelastic neutrino-nucleus scattering cross section for ^{203}Tl (left) and ^{205}Tl (right).
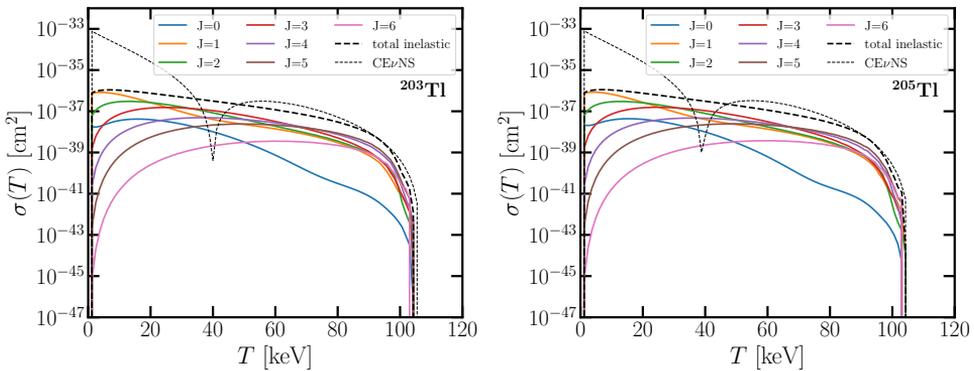

Figure 3. Inelastic scattering cross sections as functions of nuclear recoil energy for ^{203}Tl (left) and ^{205}Tl (right), showing individual J-transition contributions and comparison with CEνNS.

Fig. 3 illustrates the inelastic scattering cross sections as functions of nuclear recoil energy for both thallium isotopes. The $J = 1$ transitions dominate at low recoil energies ($T < 10$ keV), while $J = 2$ and $J = 3$ transitions become important at intermediate energies ($20 \lesssim T \lesssim 70$ keV). At higher

recoil energies, $J = 4$ and $J = 5$ transitions contribute significantly. Notably, the inelastic cross section becomes comparable to CEνNS around $T \simeq 40$ keV, where coherence loss occurs in the elastic channel due to the suppression of the nuclear form factor.

We now present our predictions for the case of actual signals expected at terrestrial detectors, by assuming solar, π-DAR and DSNB neutrinos. The left panel of Fig. 4 shows a comparison between the results obtained using the hybrid model and the NSM for the case of solar neutrino scattering. While low-energy neutrino sources (CNO, *pep*) show identical results between models, significant differences appear for ^{8}B and *hep* neutrinos in the recoil energy range $0.1 \lesssim T \lesssim 1$ keV. This enhancement stems from a spin-flip M1 giant resonance around 7.4 MeV as shown in the right panel of Fig. 4. This resonance is entirely absent in NSM calculations due to inherent model limitations. As the NSM is incapable of describing such excitations, their effect needs to be taken into account separately in pure NSM calculations. In this sense, the hybrid model can be thought of as an extension of this procedure, where instead of adding just a single important state, the hybrid approach replaces an entire energy range with more accurate states that the NSM cannot model. As a consequence the integrated event rates indicate that the hybrid model predicts roughly twice as many events compared to NSM-only calculations.
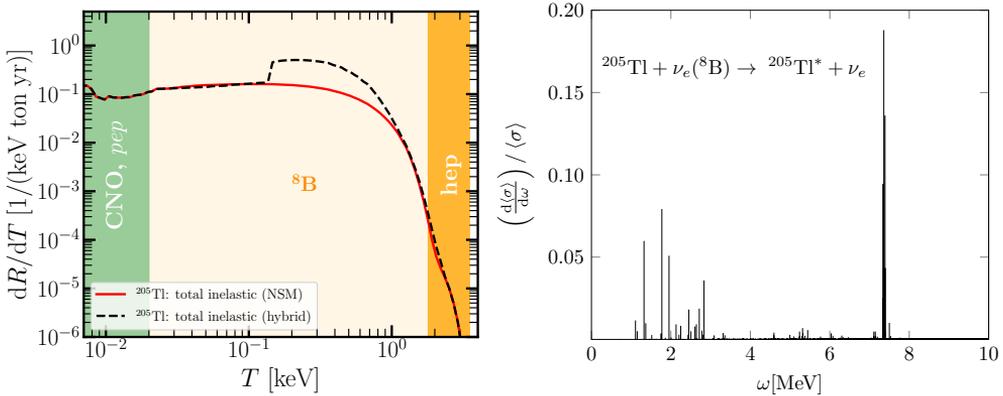

Figure 4. Left: Comparison of solar neutrino event rates between hybrid model (solid) and pure NSM (dashed) for ^{205}Tl. The hybrid model shows enhanced rates due to inclusion of high-energy nuclear states. Right: contributions from individual final nuclear states to the total folded ^{8}B solar neutrino scattering cross section off ^{205}Tl.

Finally, Figs. 5 and 6 depict the corresponding event rates for π-DAR and DSNB neutrinos, respectively, calculated using the hybrid model. The left (right) panels show the differential (integrated) spectra. It is noteworthy that while inelastic scattering remains subdominant to CEνNS for π-DAR neutrinos, the difference is much smaller than in the case of solar neutrinos. Interestingly, for DSNB, the inelastic channel becomes competitive with CEνNS at recoil energies $T \gtrsim 20$ keV. The DSNB results are particularly interesting as they represent the first calculation of inelastic rates for this astrophysical source. More importantly, the ν_x component dominates the inelastic channel at higher recoil energies, hence further motivating the present work.

The theoretical uncertainties associated with the results are difficult to quantify, as they arise mostly from the nuclear model inputs. The precise value of the energy cutoff of NSM and MQPM states presents a challenge, and we have chosen a reasonable cutoff and verified that no highly-contributing state is excluded or double-counted. Future work will focus on establishing a more well-founded method of choosing the cutoff. The nuclear many-body deficiency (NMBD) arising due to the limitations of the chosen nuclear models and interactions also affects the uncertainties. Data for NC reactions is scarce, but charged-current (CC) studies have found that despite the different typical
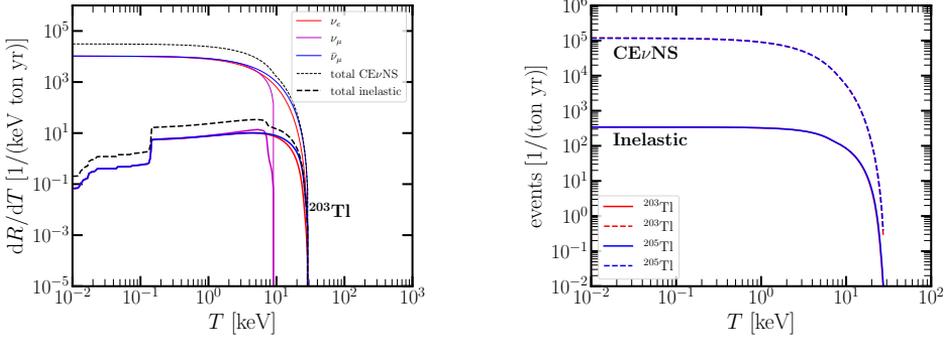
Figure 5. Differential (left) and integrated (right) number of events above threshold for inelastic π-DAR neutrino scattering off $^{203/205}$Tl nuclei using the hybrid model. The results are given for the individual neutrino flavors and their sum. The corresponding CEνNS spectra are also shown for comparison.
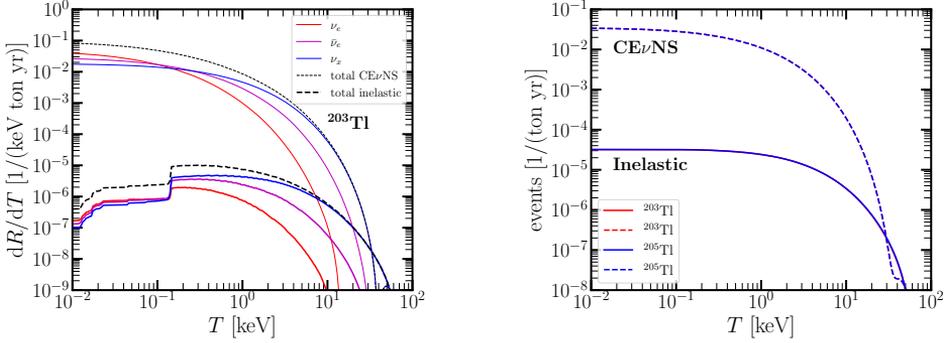

Figure 6. Same as Fig. 5, but for the case of DSNB neutrinos.

model spaces in NSM and MQPM calculations, their NMBDs seem to be of comparable size [15].

4. Conclusions

We have presented a comprehensive study of inelastic neutrino-nucleus scattering off $^{203/205}$Tl using a novel hybrid nuclear model combining the best features of NSM and MQPM. The hybrid approach demonstrates considerable promise for future neutrino scattering studies, particularly for next-generation experiments requiring accurate nuclear structure inputs across wide energy ranges. Moreover, the recoil-energy formalism provides a direct link to experimental observables. Future work will extend this approach to CC-processes and other semi-leptonic nuclear reactions. Key findings of this study include the following aspects: The hybrid model provides improved accuracy for higher-energy neutrino sources while maintaining precision for low-energy transitions. Inelastic channels become competitive with CEνNS at specific recoil energies, particularly around 40 keV where coherence is lost. For solar neutrinos, the hybrid model predicts roughly twice as many events compared to NSM-only calculation. π-DAR and DSNB neutrinos show significant inelastic contributions, with DSNB inelastic rates approaching or even surpassing CEνNS at higher recoil energies.

Acknowledgements

References

[1]   D. Akimov et al. "Observation of Coherent Elastic Neutrino-Nucleus Scattering". In: *Science* 357 (2017), pp. 1123–1126. DOI: 10.1126/science.aao0990.

[2]   D. Akimov et al. "First Measurement of Coherent Elastic Neutrino-Nucleus Scattering on Argon". In: *Phys. Rev. Lett.* 126 (2021), p. 012002. DOI: 10.1103/PhysRevLett.126.012002.

[3]   J. Colaresi, J. I. Collar, T. W. Hossbach, C. M. Lewis, and K. M. Yocum. "Measurement of Coherent Elastic Neutrino-Nucleus Scattering from Reactor Antineutrinos". In: *Phys. Rev. Lett.* 129 (2022), p. 211802. DOI: 10.1103/PhysRevLett.129.211802.

[4]   N. Ackermann et al. "Direct observation of coherent elastic antineutrino–nucleus scattering". In: *Nature* 643 (2025), pp. 1229–1233. DOI: 10.1038/s41586-025-09322-2.

[5]   Zihao Bo et al. "First Indication of Solar ^{8}B Neutrinos through Coherent Elastic Neutrino-Nucleus Scattering in PandaX-4T". In: *Phys. Rev. Lett.* 133 (2024), p. 191001. DOI: 10.1103/PhysRevLett.133.191001.

[6]   Elena Aprile et al. "First Indication of Solar ^{8}B Neutrinos via Coherent Elastic Neutrino-Nucleus Scattering with XENONnT". In: *Phys. Rev. Lett.* 133 (2024), p. 191002. DOI: 10.1103/PhysRevLett.133.191002.

[7]   G. Adhikari et al. "Search for a Dark Matter-Induced Annual Modulation Signal in NaI(Tl) with the COSINE-100 Experiment". In: *Phys. Rev. Lett.* 123 (2019), p. 031302. DOI: 10.1103/PhysRevLett.123.031302.

[8]   R. Bernabei et al. "First results from DAMA/LIBRA and the combined results with DAMA/NaI". In: *Eur. Phys. J. C* 56 (2008), pp. 333–355. DOI: 10.1140/epjc/s10052-008-0662-y.

[9]   Matti Hellgren, Dimitrios K. Papoulias, and Jouni Suhonen. "Inelastic neutrino-nucleus scattering off 203/205Tl in terms of the nuclear recoil energy using a hybrid nuclear model". In: *Phys. Lett. B* 868 (2025), p. 139624. DOI: 10.1016/j.physletb.2025.139624.

[10] Dimitrios K. Papoulias, Matti Hellgren, and Jouni Suhonen. "Incoherent solar-neutrino scattering off the stable Tl isotopes". In: *Phys. Rev. C* 110 (2024), p. 034309. DOI: 10.1103/PhysRevC.110.034309.

[11] T. W. Donnelly and R. D. Peccei. "Neutral Current Effects in Nuclei". In: *Phys. Rept.* 50 (1979), p. 1. DOI: 10.1016/0370-1573(79)90010-3.

[12] J. D. Walecka. *Theoretical nuclear and subnuclear physics.* Vol. 16. 1995.

[13] E. Ydrefors, K. G. Balasi, J. Suhonen, and T. S. Kosmas. "Nuclear Responses to Supernova Neutrinos for the Stable Molybdenum Isotopes". In: *Neutrinos: Properties, Sources and Detection.* Ed. by J.P. Greene. New York: Nova Science, 2011, pp. 151–175. ISBN: 1612096506.

[14] Martin Hoferichter, Javier Menéndez, and Achim Schwenk. "Coherent elastic neutrino-nucleus scattering: EFT analysis and nuclear responses". In: *Phys. Rev. D* 102 (2020), p. 074018. DOI: 10.1103/PhysRevD.102.074018.

[15] Jouni T. Suhonen. "Value of the Axial-Vector Coupling Strength in β and $\beta\beta$ Decays: A Review". In: *Front. in Phys.* 5 (2017), p. 55. DOI: 10.3389/fphy.2017.00055.